VELOCITY SELECTION FOR IONIZATION FRONTS IN PLANAR DC GAS-DISCHARGE SYSTEM WITH HIGH-OHMIC ELECTRODE

Svetlana V. Gurevich
Institut for Theoretical Physics
Westfälische Wilhelms-Universität Münster
Germany
gurevics@uni-muenster.de

Shalva Amiranashvili
Weierstrass Institute for Applied Analysis and Stochastics
Germany
shalva@wias-berlin.de

Abstract

In this article we deal with the theoretical investigation of pattern formation in a planar dc gas-discharge system with a high-ohmic electrode. In particular, we are interested in a description of electric breakdown in the low-current Townsend mode of discharge operation. Using the adiabatic description of electrons and two-scale expansion one can show that the discharge in this mode is governed by a two-component reaction-diffusion system, which provides a quantitative system description on the macroscopic time scale. On this base ionization fronts being nontrivial solutions of this reaction-diffusion system are discussed in details. In particular, velocity and initial condition selection are investigated in one- and two spatial dimensions.

Key words

Nonlinear dynamics, reaction-diffusion systems, ionization fronts, velocity selection, gas-discharge.

1 Introduction

The understanding of complex dynamical systems is one of the most important subjects in modern physics. In particular, the spontaneous formation of patterns in the systems far from thermal equilibrium, e.g., self-organized lighting current patterns in laterally extended systems has been the subject of substantial interest over the last decades. However, the nature of pattern formation in different systems is not always clear, despite of the large variety of models developed to describe it. In particular, despite the good knowledge of the underlaying microscopic processes in plasma, the observed macroscopic patterns ,e.g., anode spots are not understood to large extent. One reason is that typically the current patterns are threedimensional objects that evolve on a time scale of a millisecond or longer. In contrast, the smallest time scale that should be taken into account, e.g., in the popular drift-diffusion approximation, is the electron travel time that is of order of 10 nanoseconds for the systems in question. A direct numerical solution of the plasma transport equations is therefore very time consuming or even impossible. The alternative is to develop an appropriate reduced discharge model.

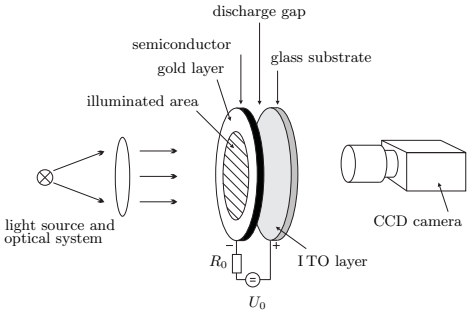

Figure 1. Schematic plot of the experimental set-up. Explanations are given in the text.

In [2] such a reduction is developed on the base of classical drift-diffusion discharge model for the planar dc gas-discharge system with a high-ohmic electorde [12; 13; 18] in low-current Townsend mode of operation. The investigated system, shown in Fig. 1, consist of a high-ohmic semiconductor cathode (chromium-doped gallium arsenide cooled to $T = 100K$) contacted from one side with a semitransparent gold layer, a gas gap of width source filled with, e.g., nitrogen at a pressure of $p \approx 300$hPa, and an indium tin oxide (ITO) anode on a glass substrate, making the anode transparent with respect to visible light. The resistivity of the semiconductor takes values of $\rho \approx 10^5 - 10^9\Omega$cm and can be controlled via the internal photo effect by illumination. The system is supplied with an external voltage U_0 of several kV, whereas the global current is limited by a series resistor R_0 of 10MΩ. The luminance distribution in the discharge gap is known to be locally proportional to the current density distribution [3] and can be recorded through the ITO electrode by a charge carrier device (CCD) camera.

When the supply voltage U_0 is increased beyond the

ignition voltage, various forms of spatially inhomogeneous self-organized luminance patterns can be observed in the discharge gap [5; 4; 10]. Here, in contrast, we concetrate on the system behaviour in low-current Townsend mode of operation.

Let us first suppose that by proper choice of the supply voltage the system is prepared to operate near to the breakdown point, that is, the voltage applied to the gas almost equals the Townsend breakdown voltage U_b. In this mode the current is negligible and is often localized in several narrow channels caused by inhomogeneities of the system. The channels serve as seed current fluctuations for the breakdown. The supply voltage is then suddenly increased to a larger value U_s, $U_s - U_b \ll U_b$. Breakdown in a system like Fig. 1 transfers it to a state that is assumed to be in the Townsend mode. In the case that the current density is uniform, it is determined by

$$j = j_0 = \frac{U_s - U_b}{\rho d_c},$$

where ρ is the specific resistivity of the high-ohmic barrier and d_c is the semiconductor width. So, the breakdown can be considered as a transition between the states with $j = 0$ and $j = j_0$.

Using adiabatic description of electrons and two-scale expansion on can demonstrate [2], that in the low-current Townsend mode the discharge is governed by a two-component reaction-diffusion system, that incorporates only radial coordinates and slow time evolution:

$$\tau_u \partial_t u = d_u^2 \nabla_\perp^2 u + uv, \qquad (1)$$

$$\tau_v \partial_t v = d_v^2 \nabla_\perp^2 v + 1 - u - v. \qquad (2)$$

Here $u = u(x, y, t)$–a normalized current density, $u = \frac{j}{j_0}$, $v = v(x, y, t)$–a normalized overvoltage, $v = \frac{\delta U}{U_s - U_b}$, τ_u, τ_v–characteristic time scales, $\tau_u = \tau_i/s$, $\tau_v = \tau_c$, d_u^2, d_v^2–diffusion lengthes, $d_u = \sqrt{\frac{\lambda_e d}{s}}$, $d_v = \frac{d_c}{\sqrt{3}}$,$s \ll 1$ is the dimensionless overvoltage parameter; λ_e is the electron diffusion length; τ_i is the ion travel time and τ_c is the RC time of the circuit (characteristic cathode time). Our goal now is to investigate the nontrivial solutions of system (1)-(2), so-called *ionization fronts*, as well as to determine which class ionization fronts belong to and find the propagating velocity. We discuss these problems below, starting with the case of one spatial dimension.

2 Ionization Fronts in 1D

For the sake of simplicity first of all let us introduce dimensionless time $t := t/d_v$ and space variables $x := x/d_v$ and rewrite the system (1, 2) in the form

$$\begin{aligned} \tau u_t &= d^2 u_{xx} + uv \\ v_t &= v_{xx} + 1 - u - v. \end{aligned} \qquad (3)$$

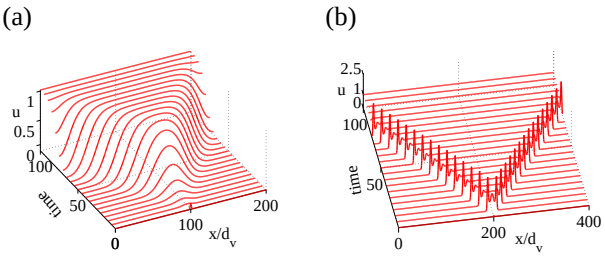

Figure 2. Numerical results [Eqs. (3)] for the form of ionization fronts for different system parameters. u mponent is presented. (a) $\tau = 5$ and $d = 4$, i.e., both time and space scales are determined by the gas; (d) $\tau = 0.2$ and $d = 0.25$, both time and space scales are determined by the cathode. In all cases the Neumann boundary conditions were used. We started from $u = v = 0$ and added a small fluctuation of u at the origin. The fluctuation quickly changes to a stable front.

where the constant d^2 denotes a ratio of the diffusion lengths $d = d_u^2/d_v^2$, whereas τ represents a ratio of the characteristic time scales and $\tau = \tau_u/\tau_v$.

The system (3) has two stationary homogeneous equilibrium solutions. The solution ($u = 0$, $v = 1$) corresponds to a vanishing current and peak overvoltage, and is referred to as the *overvoltage state*. The second solution ($u = 1$, $v = 0$) describes a stationary *Townsend state*.

The non-uniform breakdown, as a possible solution of Eqs. (3), occurs in the form of *ionization fronts*. They turn out to be transition waves between unstable and stable system states that propagates along the electrodes. In the literature propagation of such fronts is often referred to as *a front propagation into unstable state* [7; 17]. Such fronts arise in different physical systems. Here we only mention Rayleigh-Bénard [9] convection or dielectric breakdown fronts [8]. Although most of the fronts mentioned above are described by a one-component nonlinear diffusion equation, two component models can also be found [8; 15].

In the general case of Eqs. (3) no analytical solutions can be found and the numerical solutions are instead referred to. A small local initial current fluctuation leads to an exponential increase in the current. Furthermore, the instability develops in a nonlinear way: an ionization front propagates away from the initial perturbation. Finally the uniform state with $j = j_0$ ($u = 1$, $v = 0$) is established on the whole electrodes area, but plasma edges where boundary conditions affect the final current distribution. Two typical examples of front behavior for different parameters d and τ of the system are shown in Fig. 2. Space-time plots for the u-component are presented. One can see that in addition to monotonic fronts (Fig. 2 (a)), oscillating fronts can be observed (see Fig. 2 (b)). More complicated scenarios appear if there is more than one initial fluctuation. Several fronts are produced, they collide and merge with each other in the course of the collision process. At the end, however, we always have only one front that transforms the system into the uniform Townsend state. Numerical

simulations of the system (3) show that the evolution to the stationary Townsend state ($u = 1$, $v = 0$) can be either monotonic or oscillatory. So, our next goal is to determine for which system parameters (d and τ) the system produce these regimes. To this end let us move to a frame moving with a constant velocity $\xi = x - ct$,

$$d^2 u_{\xi\xi} + \tau c u_\xi + uv = u_t$$
$$v_{\xi\xi} + c v_\xi + 1 - u - v = v_t,$$

where $u = u(\xi, t), v = v(\xi, t)$.

Let us consider a stationary solution of this system and a small perturbation of the stationary solution $\widetilde{\mathbf{u}} = (\widetilde{u}, \widetilde{v})$, i.e., $u = 1 + \tilde{u}$, $v = 0 + \tilde{v}$. Then the equation for $(\widetilde{u}, \widetilde{v})$ becomes:

$$d^2 \widetilde{u}_{\xi\xi} + \tau c \widetilde{u}_\xi + \widetilde{v} = 0$$
$$\widetilde{v}_{\xi\xi} + c\widetilde{v}_\xi - \widetilde{u} - \widetilde{v} = 0,$$

After decomposing $\widetilde{\mathbf{u}}$ into modes $\widetilde{\mathbf{u}} \sim \mathbf{a} e^{\lambda\xi}$, $\lambda \in \mathbb{C}$ we get the equation

$$A_\lambda \mathbf{a} = 0 \tag{4}$$

with

$$A_\lambda = \begin{pmatrix} \lambda^2 d^2 + \tau c\lambda & 1 \\ -1 & \lambda^2 + c\lambda - 1 \end{pmatrix}.$$

The system (4) allows for a nontrivial solution if a compatibility condition

$$\det(A_\lambda) = d^2\lambda^4 + c(d^2+\tau)\lambda^3 + (\tau c^2 - d^2)\lambda^2 - \tau c\lambda + 1 = 0 \tag{5}$$

holds. This equation is a polynomial of the fourth order, so it can possesses at most four roots, which, depending on coefficients, can be either complex or real. If $\mathrm{Im}(\lambda) = 0$ the ionization front is monotonic and is oscillatory otherwise. So, if we know the velocity for given d and τ one can define the front behavior, analyzing $\mathrm{Im}(\lambda)$.

In order to calculate the front velocity numerically, one can, for example, derive the current as an integral of the $u = j/j_0$ over a space. Then one can obtain the front velocity as time derivative of this integral. An example of two typical front velocities corresponding to four different front types is shown in Fig. 3. One can see that for different system parameters the front velocity are of two orders of magnitude. Moreover, oscillating fronts move faster than monotonic fronts. Although the velocity of the ionization front is simple to find numerically, the question arises, whether some analytical results can be obtained? This problem is discussed in detail in the next section.

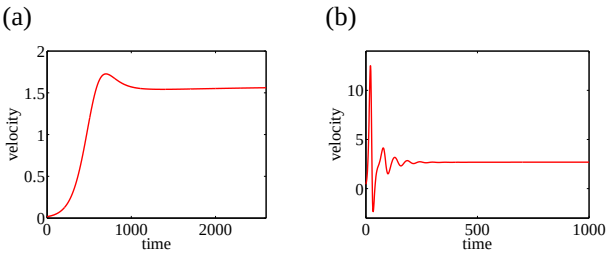

Figure 3. Velocities of ionization fronts calculated for four typical front forms as a function of a time: (a) $d = 4, \tau = 5$, monotonic front; (b) $d = 0.25, \tau = 0.2$, oscillating front. Initially the front velocity increases in time, what corresponds to the region, where the ionization front is formed. After the front formation the velocity converges to the constant value, depending on system parameters.

3 Velocity selection problem

Suppose that initially the system is in an unstable state except of some spatially localized region. The question is, what will be the long-time ($t \to \infty$) dynamical properties and velocity of the nonlinear front which will propagate into the unstable state? Are there classes of initial conditions for which the front converges to some unique asymptotic state c^*? If so, what can be said about the asymptotic front properties and convergence to them?

To address these questions, let us linearize the basic system (3) about the unstable state $u = 0, v = 1$. The linearized system reads:

$$\tau \widetilde{u}_t = d^2 \widetilde{u}_{xx} + \widetilde{u}$$
$$\widetilde{v}_t = \widetilde{v}_{xx} - \widetilde{u} - \widetilde{v}, \tag{6}$$

where $(\widetilde{u},\ \widetilde{v})$ are the small perturbations of $u = 0,\ v = 1$, i.e., $u = 0 + \widetilde{u},\ v = 1 + \widetilde{v}$. From this point on we will have to deal only with the first equation of (6), because it is not coupled with $\widetilde{v}$. This equation is a linear diffusion equation with a source term, well known in the literature. Moreover, it is identical to the linearization of the classical nonlinear diffusion equation investigated by Fisher and Kolmogorov [16; 7; 17]. So one can try to apply the classical methods and results to the system (3).

Due to linearity of the equation for u for long times the profile in the leading edge will take the form $\widetilde{u} \sim \exp(ikx - i\omega t)$, where $\omega = \omega(k)$ is a dispersion function,

$$\omega(k) = \frac{\imath(1 - d^2k^2)}{\tau}. \tag{7}$$

Notice that k and $\omega(k)$ can be complex: $k_i := \mathrm{Im}(k)$ is associated with the spatial decay of the front envelope and $k_r := \mathrm{Re}(k)$ with the oscillations, since $\mathrm{Re}(e^{\imath kx}) = e^{-\mathrm{Im}(kx)} \cos\big(\mathrm{Re}(kx)\big)$.

Since k is in general complex, the dynamical selection of both its real and complex parts must be analyzed.

The selection of a particular "mode" $\mathrm{Re}(k)$ can be understood as follows: For fixed values of $k_i = k_{i0}$ the growth rate $\omega_i := \mathrm{Im}(\omega(k))$ is a function of k_r only and has a maximum at $k_r = 0$. Hence if one considers a superposition of profiles of the form $\exp(ikx - i\omega t)$ with the same value of the spatial decay $k_i = k_i^\dagger$, the long-time appearance of the profile will be dominated by the mode k_r corresponding to the $\max(\omega_i)$, i.e., for which $\partial\omega_i/\partial k_r = 0$ and $\partial^2\omega_i/\partial k_r^2 < 0$. So, in order to understand the selection of the spatial decay rate k_i it is enough to consider for each value of k_i only the maximum rate mode. In other words, k_r is considered to be an implicit function of k_i through the condition $\partial\omega_i/\partial k_r = 0$. Thus the envelope velocity

$$c := c(k_i) = \frac{\omega_i}{k_i} = \frac{1}{\tau k_i} + \frac{d^2 k}{\tau} \qquad (8)$$

is the function of k_i only. As can be seen from Eq. (8) the envelope velocity is a parabola-like function with a minimum at $k_i^{min} = 1/d$. Let us first check the stability of both branches of this function described by Eq. (8). For this aim we move to the frame moving with the envelope velocity $\xi = x - ct$. In the leading edge region $\widetilde{u} \sim \alpha(t)\exp(-k_i\xi)$, where the spatial decay $k_i \geq 0$, so one obtaines

$$\dot{\alpha}(t) = \left(\frac{d^2}{\tau}k_i^2 - ck_i + \frac{1}{\tau}\right)\alpha(t).$$

Then the stability conditions for c are

$$k_i \geq 0$$
$$f(k_i, c) = \frac{d^2}{\tau}k_i^2 - ck_i + \frac{1}{\tau} \leq 0;$$

It is easy to show that the latter conditions are satisfied if $f(k_i^*, c) \leq 0$, where $k_i^* = c\tau/2d^2$ is a minimum of the function $f(k_i, c)$. In its turn, the inequality $f(k_i^*, c) \leq 0$ is satisfied if and only if $c \geq 2d/\tau$. Thus, the envelope velocity is stable only on the left branch of the parabola (8), i.e., for $k_i \leq 1/d$. To understand the essence of the dynamical mechanism of the velocity selection let us imagine a hypothetical front consisting of two pieces of the form $\exp(\imath kx - \imath\omega t)$ with two different values of k_i and velocities c (see Fig. 4 (a)). As sketched in Fig. 4, the line drawn with a red line drops off slower than the blue piece, as $k_a < k_b$ (see Fig. 4 (a, b)). On the other hand, as Fig. 4 (a) indicates, the red profile moves faster than the blue ones ($c_a > c_b$). Nevertheless, as Fig. 4 (b) demonstrates, the slowest moving part of the profile expands in time, i.e., becomes dynamically dominant. That is, for $t \to \infty$ the velocity $c^* = 2d/\tau$, corresponding to the smallest wave number $k_i^{min} = 1/d$ is seems to be selected.

Notice, that this conclusion is based on two facts, namely (a) the fastest profile has the slowest spatial decay and (b) the fact that the part with the fastest spatial

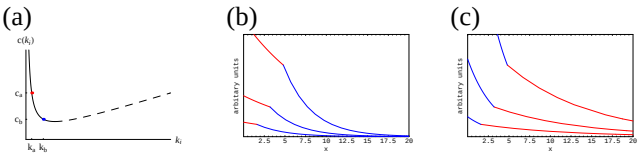

Figure 4. Intuitive illustration of velocity selection. (a) Typical behavior of $c(k_i)$. The behavior of the fronts, corresponding to points $(k_a,\ c_a)$ and $(k_b,\ c_b)$ are shown in figures (b) and (c); (b) The lower part of the envelope of a front profile, drawn with a blue line corresponding to the point $(k_b,\ c_b)$ in figure (a). It moves slower as a red line, corresponding to $(k_a,\ c_a)$, but falls off steeper. The figure demonstrates how the crossover point moves higher with time, so that the profile becomes dominated by the slowly moving part; (c) If the slowest profile with $(k_b,\ c_b)$ is not one to the right, the fastest profile emerges.

decay is *to the right* of the one with the slower spatial decay. That is, the slowest profile dominates because it is in front of the faster one. Indeed, if both lines are interchanged so that the faster one is to the right, as shown in Fig. 4 (c), the faster one dominates the long-time dynamics.

These observations imply that initial conditions are important: only if the initial condition profile $u(x, 0)$ drops off faster than $\exp(-k_i^{min}x)$ the asymptotic front velocity is equal to the minimum value of (8), i.e., $c^* = 2d/\tau$. Otherwise, if $u(x, 0) \sim \exp(-\alpha x)$, where $\alpha \leq k_i^{min}$, the asymptotic velocity is simply

$$c = c(\alpha) = \frac{d^2\alpha}{\tau} + \frac{1}{\tau\alpha} > c^*.$$

In the former case the initial condition is refereed to as *sufficiently localized* whereas in the latter case they are said to be *flat* [7].

In the following the initial conditions are assumed to be sufficiently localized. In this case, as discussed above, the asymptotic velocity is given by

$$c^* = \frac{\omega_i}{k_i} = \frac{2d}{\tau}, \qquad \frac{\partial\omega_i}{\partial k_r} = 0, \qquad \frac{\partial^2\omega_i}{\partial k_r^2} < 0. \quad (9)$$

These equations determine *the linear-marginal stable velocity* c^* as well as the wave number k_i^{min} at that point. The corresponding front is said to be *pulled* or *marginally stable* [6; 16; 7]. The analysis shows why the front velocity approaching the asymptotic value is based on the assumption that the dynamically relevant branch of $c(k_i)$ corresponds to the smallest root k_i^{min} for solving the equation (9). This occurs because an asymptotic spatial decay

$$\widetilde{u} \simeq \sum_j A_j(c)e^{-\imath k_i^j x}$$

will be dominated by the root with the smallest value of k_i, say, $k_i^{min} = k_i^1$, whenever the corresponding factor

$A_1(c) \neq 0$. Nevertheless, it may happen that at some particular value $c^\dagger$ one has

$$A_1(c^\dagger) = 0, \tag{10}$$

so that asymptotic spatial decay is not given by $k_i^{min} = k_i^1$, but instead by the next root with $k_i^2 > k_i^1$. The dynamical implications of this can be understood immediately within the same context as those used for the case of linear marginal stability. Namely, the front moving with a velocity $c^\dagger$ drops off faster in space than any other front profile with velocity $c > c^*$. On the other hand if the velocity $c^\dagger$ satisfies Eq. (10), all fronts with $c < c^\dagger$ are unstable against "invasion" by the profile with $c^\dagger$ and the asymptotic front velocity for sufficient localized initial conditions becomes $c^\dagger$. So, $c^\dagger$ is also the velocity at which front profiles are *marginaly stable*. However, in this case the smallest root k_i^{min} does not dominate the asymptotic spatial decay of the front profile and the asymptotic front behavior depends on the properties of the whole front. Therefore the velocity $c^\dagger$ is referred to as *the nonlinear marginal velocity* and the corresponding front profile is said to be $pushed$ following [16; 7].

Although the physical understanding for the nonlinear marginal stability described above is quite simple, the analytical prediction of $c^\dagger$ is much more complicated. However, sometimes it is possible to do for nonlinear diffusion equation with some spatial type of nonlinear term [16]. For the system (3) we refer to a numerical solution.

The system (3) shows that both pulled and pushed fronts can be found. Numerical simulations show that monotonic fronts, occurring in (3) are pulled, whereas the oscillatory ones are pushed. In [7] it has been proven that for nonlinear diffusion equation monotonic fronts propagating with the asymptotic velocity c^* are stable, what is in agreement with our numerical results.

4 Ionization fronts in 2D

Qualitatively, the behavior of the general solution in two-dimensional space is the same as in one-dimension. An initial current perturbation changes to stable ionization front. The latter propagates away from the initial perturbation and quickly changes to a quasi-one-dimensional front. The structure of the transition region is also the same as in the one-dimensional case: apart from monotonic fronts, oscillatory behavior can also be found. An example of both front types is shown in Fig. 5 Figure 5 (a) shows a cross-section of the two-dimensional monotonic front for a fixed time moment. The red surface presents the $u = j/j_0$ distribution, whereas the blue surface describes the overvoltage v. An example of the oscillatory front is shown in Fig. 5 (b). As in the case of one dimension the fronts move with a constant velocity, that depends on system parameters and is independent on initial fluctuation if it is well-localized. In contrast to the one-dimensional front, the velocity in two-dimensions depends also on the front curvature. On the other hand, the two-dimensional front rather quickly changes to a quasi-one-dimensional front, moving with the asymptotic velocity c^* for monotonic and $c^\dagger$ for oscillatory fronts.

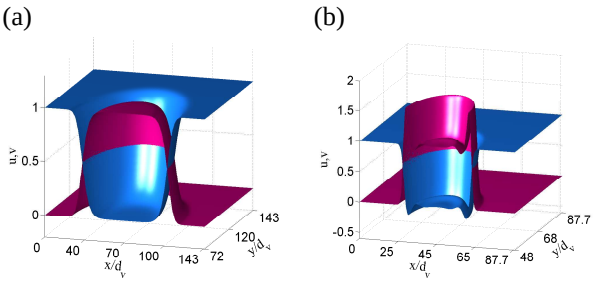

Figure 5. Two dimensional ionization fronts. $u = u(x, y, t)$ (red) as well as $v = v(x, y, t)$ (blue) distributions are shown. (a) monotonic front, calculated at $t = 1500$. Parameters: $d = 5.2/3.5, \tau = 4.5/0.91, L = [0, 143] \times [0, 143], dx = 0.01, dt = 0.03$; (b) oscillatory front, calculated at $t = 1100$. Parameters: $d = 1.7/5.7, \tau = 4.1/9.7, L = [0, 87.7] \times [0, 87.7], dx = 0.01, dt = 0.03$. In both cases the Neumann boundary conditions were used.

In the case of several initial fluctuations, the front behavior is also similar to the one-dimensional case: several fronts are produced, they collide and merge with each other throughout the collision process. At the end, however, there is only a single front that transforms the system into the uniform Townsend state.

5 Conclusion

We investigated electric breakdown and transition to the Townsend discharge mode for a gaseous plane-parallel discharge cell. The key problem is that the experimental phenomena are observed on a macroscopic time scale (of the order of 10^{-3} s or longer), whereas the drift-diffusion approximation is on a microscopic time scale. A direct numerical solution of the full 3D drift-diffusion equations on macroscopical time scales is very time consuming or even impossible and a reduction of the drift-diffusion model is desirable. Such a reduction is developed using the fact that the axial dimension of the discharge cell in question is small as compared to the radial dimension [2]. Two-scale approach allows the axial and radial effects to be separated. The resulting two-component reation-diffusion system possesses nontrivial solutions in form of ionization fronts. Under certain system parameters the one- and two-dimensional ionization fronts can be either monotone or oscillatory and move with a constant velocity. This velocity depends on front type and the initial distribution. Moreover, if the initial conditions are well-localized monotone fronts always move with the asymptotic marginal stable velocity c^*, which can be found analytically. In contrast, oscillatory fronts move with constant velocity $c^\dagger > c^*$, which are called

to be nonlinear marginally stable and for the system in question can be found numerically. If the initial distribution is not sufficiently well-localized (flat) the front velocity depends on the initial distribution and system parameters.

References

G. Ahlers and D. S. Cannell. Vortex-front propagation in rotating couette-taylor flow. *Phys. Rev. Lett.*, 50:1583, 1983.

Sh. Amiranashvili, S. V. Gurevich, and H.-G. Purwins. Ionization fronts in planar dc discharge systems with high-ohmic elctrode. *Physical Review E*, 71:066404, 2005.

E. Ammelt, Yu. A. Astrov, and H.-G. Purwins. Stripe turing structures in a two-dimensional gas discharge system. *Physical Review E*, 55(6):6731–6740, 1997.

E. Ammelt, Yu. A. Astrov, and H. G. Purwins. Hexagon structures in a two-dimensional DC-driven gas discharge system. *Physical Review E*, 58(6):7109–7117, 1998.

Y. A. Astrov and Y. A. Logvin. Formation of clusters of localized states in a gas discharge system via a self-completion scenario. *Physical Review Letters*, 79(16):2983–2986, 1997.

E. Ben-Jacob, H. Brand, G. Dee, L. Kramer, and J. S. Langer. Pattern propagation in nonlinear dissipative systems. *Physica D*, 14:348–364, 1985.

U. Ebert and W. van Saarloos. Front propagation into unstable states: universal algebraic convergence towards uniformly translating pulled fronts. *Physica D*, 146:1–99, 2000.

U. Ebert, W. van Saarloos, and C. Caroli. Streamer propagation as a pattern formation problem: Planar fronts. *Phys. Rev. Lett.*, 77:4178, 1996.

J. Fineberg and V. Steinberg. Vortex-front propagation in rayleigh-bénard convection. *Phys. Rev. Lett.*, 58:1332, 1987.

E. L. Gurevich, A. S. Moskalenko, A. L. Zanin, Yu. A. Astrov, and H.-G. Purwins. Rotating waves in a planar dc-driven gas-discharge system with semi-insulating gaas cathode. *Physics Letters A*, 307(5-6):299–303, 2003.

J. D. Murray. *Mathematical Biology*. Springer, Berlin, 1993.

H.-G. Purwins, G. Klempt, and J. Berkemeier. Temporal and spatial structures of nonlinear dynamical systems. *Festkörperprobleme*, 27:27–61, 1987.

H.-G. Purwins, C. Radehaus, and J. Berkemeier. Experimental investigation of spatial pattern formation in physical systems of activator-inhibitor type. *Zeitschrift für Naturforschung*, 43a(1):17–29, 1988.

E. K. H. Salje. On the kinetics of partially conserved order parameters: a possible mechanism for pattern formation. *J. Phys. Condens. Matter*, 5:4775, 1993.

S. Theodorakis and E. Leontidis. Speed selection mechanism for propagating fronts in reaction-diffusion systems with multiple fields. *Phys. Rev. E*, 65:026122, 2002.

W. van Saarloos. Front propagation into unstable states. ii. linear versus nonlinear marginal stability and rate of convergence. *Phys. Rev. A*, 39:6367, 1989.

W. van Saarloos. Front propagation into unstable states. *Physics Reports*, 386:29–222, 2003.

H. Willebrand, C. Radehaus, F.-J. Niedernostheide, R. Dohmen, and H.-G. Purwins. Observation of solitary filaments and spatially periodic patterns in a DC gas -discharge system. *Physics Letters A*, 149:131–138, 1990.